AR-010-236

DSTO

Development and Validation of a Finite Element Based Method to Determine Thermally Induced Stresses in Bonded Joints of Dissimilar Materials

R.J. Callinan, S. Sanderson,
T. Tran-Cong and K. Walker

DSTO-RR-0109

APPROVED FOR PUBLIC RELEASE

DEPARTMENT OF DEFENCE
DEFENCE SCIENCE AND TECHNOLOGY ORGANISATION

Development and Validation of a Finite Element Based Method to Determine Thermally Induced Stresses in Bonded Joints of Dissimilar Materials

R.J.Callinan, S. Sanderson, T. Tran-Cong and K.Walker

Airframes and Engines Division
Aeronautical and Maritime Research Laboratory

DSTO-RR-0109

ABSTRACT

A validation is carried out of the steady state thermal stress analysis capability of the PAFEC Finite Element program. Two problems are considered for which closed form solutions can be obtained: these comprise the thermal stresses in a heated circular plate and also a bonded joint. Also, a procedure is developed for calculation of residual stresses in bonded joints. Comparisons with closed form solutions indicate the degree of discretisation necessary to achieve accurate results.

RELEASE LIMITATION

Approved for public release

DEPARTMENT OF DEFENCE

DEFENCE SCIENCE AND TECHNOLOGY ORGANISATION

Published by

DSTO Aeronautical and Maritime Research Laboratory
PO Box 4331
Melbourne Victoria 3001 Australia

Telephone: (03) 9626 7000
Fax: (03) 9626 7999

AR-010-236
June 1997

APPROVED FOR PUBLIC RELEASE

Development and Validation of a Finite Element Based Method to Determine Thermally Induced Stresses in Bonded Joints of Dissimilar Materials

Executive Summary

Accurate computational thermal stress analysis is particularly important for assessment of the viability of bonded repairs to military aircraft. Thermal stresses arise due to the different coefficients of thermal expansion of the materials involved and may be significant at the extremes of the operating temperatures of these aircraft. Furthermore it is known that the residual thermal stresses due to the bonding process may be significant. Previously, the thermal stress capability of the PAFEC Finite Element program has not been used at AMRL. Also no PAFEC steady state temperature test problems are available. As a result it has been necessary to carry out tests for which closed form solutions can be obtained. The problems considered are the thermal stresses in a heated circular plate and a bonded joint. Furthermore an algorithm is developed for the calculation of residual stress. Results obtained show that the procedures developed here give an accurate assessment of the thermally induced stress state in bonded joints. The algorithm developed can be applied to more complex geometries to enable a full assessment of the thermal stress aspects of bonded repairs.

Authors

R.J. Callinan
Airframes and Engines Division

Mr. R.J.Callinan is a senor research scientist and graduated from RMIT (Aero. Eng.) in 1969 and from Monash University in 1971 (Civil. Eng.) and completed a M.Eng. Sc. in 1981 at Melbourne University. His work has been in the areas of finite element analysis, fracture mechanics and structural mechanics of composite and bonded repairs, and military aircraft accident investigations. He has also been involved with design studies of low radar cross-section battlefield surveillance R.P.V.'s. In 1985 he was seconded to the USAF at Eglin AFB for 18 months, to carry out vulnerability studies on composite structures.

S. Sanderson
Airframes and Engines Division

Mr. Sanderson has worked at AMRL since 1981. He has developed flight data reduction & analysis software for Mirage, F-111 & F/A-18 projects. Several of these programs have been implemented by NAE for their data reduction in the IFOST project. Since 1992 Mr.Sanderson has been involved with the F.E. analysis of composite and bonded structures for F-111 & F/A-18.

T. Tran-Cong
Airframes and Engines Division

Dr Ton Tran-Cong completed a Phd at Sydney University in 1977. He has been at AMRL since 1981 and has been working in the area of linear elasticity.

K. Walker
Airframes and Engines Division

Mr Walker graduated in 1983 with a Bachelor of Aeronautical Engineering (with distinction) from RMIT. He then served for eight years with the RAAF, including a posting to the USA where he gained a Masters of Science in Aeronautics and Astronautics from Purdue University. He then worked for three years in private industry before joining AMRL in early 1994. His work at AMRL has included fatigue and damage tolerance analysis studies and aircraft load spectrum determination using the Aircraft Fatigue Data Analysis System (AFDAS). He is currently also task manager "Analysis and Validation of Design Procedures for Bonded Repairs".

Contents

Notation

k	ply number in laminate
n	total number of plies in laminate
r	radius
s	stiffness ratio
t	thickness of laminate
t_0	thickness of inner region of circular plate
t_1	thickness of plate
t_2	thickness of patch
t_a	thickness of adhesive
u_0	displacement of inner region of circular plate
u_1	displacement in outer region in circular plate
u_1	displacement in 1D bonded joint
u_2	displacement in patch on circular plate
u_2	displacement of reinforcement in 1D bonded joint
x	Cartesian co-ordinate
y	Cartesian co-ordinate
z	Cartesian co-ordinate
C_1	constant of integration
C_2	constant of integration
C_3	constant of integration
E	Young's modulus
E_0	Young's modulus for inner region of circular plate
E_1	Young's modulus in circular plate
E_2	Young's modulus in patch on circular plate
E_{11}	Young's modulus orthotropic material in 1 direction
E_{22}	Young's modulus orthotropic material in 2 direction
G	shear modulus
G_a	shear modulus of adhesive
R_I	inner radius of circular plate
R_O	outer radius of circular plate
T_I	temperature of inner region
T_O	temperature at outer radius

Notation continued

α coefficient of thermal expansion
α_0 coefficient of thermal expansion of inner region of circular plate
α_1 coefficient of thermal expansion of circular plate
α_1 coefficient of thermal expansion of component 1 in 1D bonded joint
α_2 coefficient of thermal expansion of patch on circular plate
α_2 coefficient of thermal expansion of reinforcement in 1D bonded joint
α_L longitudinal coefficient of thermal expansion of laminate
α_T transverse coefficient of thermal expansion of laminate
α_{eff} effective coefficient of thermal expansion of circular plate
ν Poisson's ratio in isotropic material
ν_{12} Poisson's ratio for contraction in 2 direction associated with extension in 1 direction
ν_{21} Poisson's ratio for contraction in 1 direction associated with extension in 2 direction
σ direct stress
σ_a applied stress to bonded joint
σ_0 radial stress in inner region of circular plate
σ_1 radial stress in circular plate
σ_1 direct stress in 1D bonded joint
σ_2 radial stress in patch on circular plate
σ_2 direct stress in reinforcement of 1D bonded joint
ε_r radial strain
τ shear stress in 1D bonded joint
τ_{max} maximum shear stress in 1D bonded joint
θ angle of k^{th} ply to longitudinal axes

[B] relates strains to displacements
[C] conductivity matrix
[D] elasticity matrix
[K] stiffness matrix
{d} displacement vector
{P} load vector
$\{P_T\}$ thermal load vector
{Q} heat flux vector
{T} nodal temperature vector
∇^2 Laplacian operator

1. Introduction

In this report comparisons are made between the F.E. results for a number of thermal stress solutions and closed form solutions. The thermal stress options for the PAFEC F.E. program have not been previously used at AMRL and a validation of these solutions is required. While standard test data files are available for transient analysis, no steady state only test problems exist. To gain confidence in the results it is necessary to validate the solutions. The most useful solutions are those for which differential equation solutions exist. In this paper the heated circular plate is analysed since the closed form solution is available, and also this will validate a two dimensional analysis. The solution for the adhesive shear stress in a bonded joint will also be considered. Furthermore the F.E. method will be applied to a residual stress problem for which an analytic solution is available.

2. Finite Element Thermal Stress Analysis

A thermal stress analysis is usually carried out with the intention to calculate thermally induced stresses, strains or displacements. Thermal stresses may arise, for example, in a bonded joint consisting of materials with different thermal coefficients of thermal expansion. Thermal stresses may occur in a heated structure which is rigidly constrained, and also in a structure with temperature gradients. Thermal stress analysis is usually carried out in two steps, the first being the thermal analysis which will calculate temperatures at each node, and the second to calculate the corresponding stresses and displacements.

The simplest thermal analysis is that of steady state temperature or steady state conduction. In this case the equations are linear and are derived from the Laplace relationship and in matrix form are:

$$[C]\{T\} = \{Q\} \qquad ...(1)$$

where:

$[C]$ is the conductivity matrix

$\{T\}$ is the nodal temperature vector

$\{Q\}$ is the heat flux vector.

The boundary conditions may be specified as temperatures or heat flux at nodes. A partitioning of equation (1) is carried out into unknown and known temperatures. If the heat flux is known at a node, then the temperature is treated as being unknown at that node. The thermal solution carried out by PAFEC uses 'thermal' elements whose properties are dependent on the geometry and thermal conductivity for that material. This analysis solves for the temperature vector and writes it to a file for use in the structural analysis which follows.

The static structural solution involves the matrix equations:

$$[K]\{d\} = \{P\} + \{P_T\} \qquad ...(2)$$

where:

$[K]$ is the structure stiffness matrix
$\{d\}$ is the displacement vector
$\{P\}$ is the applied load
$\{P_T\}$ is the thermal load vector and is given by:

$$\{P_T\} = \int [B][D][\alpha]\{T\}dv \qquad ...(3)$$

where:

$[B]$ relates strains to displacements
$[D]$ is the elasticity matrix
$[\alpha]$ are the coefficients of expansion
$[T]$ is the temperature vector from the thermal solution
dv integration is taken over the volume.

The thermal load vector is added to any applied loads that exist, and the usual displacement solution is obtained. This corresponds to the second PAFEC run in which the previously calculated temperatures are read back in.

3. Heating of a circular plate

Consider now a circular plate shown in Fig. 1. This plate is uniformly heated within a radius $r = R_I$ equal to a temperature T_I, while the temperature at the boundary is T_O. The temperature solution given in ref(1) which satisfies the Laplacian operator:

$$\nabla^2 T = 0 \qquad ...(4)$$

is given by:

$$T = T_O + \frac{(T_I - T_O)\ln(r / R_O)}{\ln(R_I / R_O)} \text{ for } R_I \le r \le R_O \text{ and}$$
$$T = T_I \qquad \text{for } r \le R_I \qquad ...(5)$$

For this temperature distribution, the following differential equation, ref(2), is applicable to plane stress:

$$\frac{d}{dr}\left(\frac{1}{r}\right)\frac{d(ru)}{dr} = \alpha(1+\nu)\frac{dT}{dr} \qquad ...(6)$$

where:

r	is the radius
u	is the radial displacement
ν	is Poisson's ratio
α	is the coefficient of thermal expansion
T	is the temperature.

For the case of plane stress, and fixed edges the strain can be defined as:

$$\varepsilon_r = \alpha_{eff}(T_I - T_O) \qquad ...(7)$$

Where α_{eff} is the effective coefficient of thermal expansion and is given by:

$$\alpha_{eff} = \frac{\alpha(1+\nu)}{R_O(T_I - T_O)}\left[R_O T - (\frac{R_O}{r^2})\int_0^r rTdr - (\frac{1}{R_O})\int_0^{R_O} rTdr\right] \qquad ...(8)$$

The explicit solution given by ref(1) for the case of fixed edges for $r \le R_I$ is:

$$\alpha_{eff} = \frac{\alpha(1+\nu)}{2}\left\{1 + \frac{1 - R_I^2 / R_O^2}{2\,ln(R_I / R_O)}\right\} \qquad ...(9)$$

As expected, the expression is dependent on the geometry only and not temperature.

Firstly a heat flow analysis is carried out using 'thermal' elements, ref(3). For the example considered here the boundary conditions are specified as $T_I = 100^oC$ at $r \le R_I$ and $T_O = 0^oC$ at $r = R_O$. Also inner radius $R_I = 162\ mm$ and outer radius $R_O = 5000\ mm$. The F.E. mesh for this case is shown in Fig.2. and indicates the discretisation necessary to give good results. Material and thermal constants are given in Tables 1 and 2. Temperatures computed from the F.E. analysis, in the radial direction, are presented in Table 3 together with results predicted from equation (5). In this case agreement has been achieved to at least four significant figures and is a validation of this part of the analysis. Also contour plots of temperature show concentric rings about $r = 0$ and confirm that the solution is radially dependent only.

The second analysis is carried out with the geometry above but with equivalent structural elements, and in this case the boundary conditions correspond to restraints around the outer circumference of the plate. A comparison between the F.E. and analytical results for α_{eff} are shown in Table 4 for a range of outer radii (R_O). The F.E. values of α_{eff} have been computed from displacements. This is necessary since in PAFEC, strains are calculated from stresses, and in the case of thermal stresses in which the structure is restrained, these strains do not correspond to real strains.

The analytic results in Table 4 are calculated from equation (9) and correspond to fixed edge conditions around the circumference. The comparison between F.E. and analytic results shows that good agreement has been obtained for $0 \le r \le R_I$. Also, contour plots of Von Mises strains show concentric rings about $r = 0$ and also indicate that the solution is radially dependent only.

The validation obtained here is particularly important. As mentioned in ref(1) the calculation of the effective coefficient of expansion in a structure is important in determining the residual stresses in a bonded structure. The effective coefficient of expansion of the plate structure is very much lower than the value α in the asymptotic limit $R_I / R_O = 0$,

i.e. $$\alpha_{eff} = \frac{\alpha(1+\nu)}{2} \qquad ...(10)$$

From equation (10) the asymptotic value for the plate is 14.95×10^{-6} and the maximum value of α_{eff} in Table 4, 12.7×10^{-6}, corresponding to the maximum radius, is still less than this value.

The lower value of the coefficient of thermal expansion, in this example, is firstly due to the circumferential restraints applied to the edge of the plate and secondly is the result of the resistance of the surrounding colder structure. This occurs, for example, in the bonding of a high strength repair to the wing of an aircraft in which a high temperature, over a local area, is required to cure the adhesive.

4. Thermal stresses in a bonded joint

4.1 1 Dimensional equation

In a bonded joint in which two materials are bonded together, thermal stresses may develop as a result of the difference in thermal coefficients of expansion. The following derivation will be given for a simple double overlap joint whose geometry is given in Fig.3 together with the location of the origin of the x axis. It is assumed that all the load transferred by the lap joint is by adhesive shear. Also, in this symmetrical joint it is assumed that no bending takes place.

The constitutive equations are:

$$\frac{du_1}{dx} = \frac{\sigma}{E_1} + \alpha_1 \Delta T \quad , \quad \frac{du_2}{dx} = \frac{\sigma_2}{E_2} + \alpha_2 \Delta T \qquad ...(11)$$

where:

u_1 and u_2 are the displacements in the components of the joint

α_1 and α_2 are the thermal coefficients of expansion

E_1 and E_2 are the Young's moduli of the two materials
ΔT is the change of temperature
σ_1 and σ_2 are the stresses in the components of the joint.

The equilibrium equations are:

$$\frac{d\sigma_1}{dx} + \frac{\tau}{t_1} = 0 \qquad \frac{d\sigma_2}{dx} - \frac{\tau}{t_2} = 0 \qquad \text{...(12)}$$

where:

t_1, t_2 are the different thicknesses of the two components and
τ is the shear stress in the adhesive.

Compatibility requires that the shear stress is given by:

$$\tau = \frac{G_a}{t_a}(u_2 - u_1) \qquad \text{...(13)}$$

where:

t_a is the thickness of the adhesive
G_a is the shear modulus of the adhesive.

Differentiating equation (13) twice, equation (11) once, and using equation (12) leads to a simple d.e.:

$$\frac{d^2\tau}{dx^2} - \frac{\tau G}{t_a}\left[\frac{1}{E_2 t_2} + \frac{1}{E_1 t_1}\right] = 0 \qquad \text{...(14)}$$

It can be shown that the solution of this equation is given by:

$$\tau = \tau_{max} e^{-x/l} \qquad \text{...(15)}$$

where: $$l = \left[\frac{t_a E_1 E_2 t_1 t_2}{G_a(E_1 t_1 + E_2 t_2)}\right]^{1/2}$$

Differentiating equation (13), equation (15) and using equation (11) leads to:

$$\tau_{max} = \frac{G_a l}{t_a}\left[\frac{\sigma_A}{E_1} + (\alpha_1 - \alpha_2)\Delta T\right] \qquad \text{...(16)}$$

For thermal stresses only $\sigma_A = 0$ and:

$$\tau = \frac{G_a l}{t_a}(\alpha_1 - \alpha_2)\Delta T e^{-x/l} \qquad ...(17)$$

The direct stress for component 1 is determined from equation (12) and equation (17), and is given by:

$$\sigma_1 = \frac{G_a l^2}{t_a t_1}\left[\frac{\sigma_A}{E_1} + (\alpha_1 - \alpha_2)\Delta T\right]\left(e^{-x/l} - 1\right) \qquad ...(18)$$

At x=0, $\sigma_1 = 0$, and σ_1 rises to a maximum value when x is large which is given by:

$$\sigma_1 = -\frac{G_a l^2}{t_a t_1}\left[\frac{\sigma_A}{E_1} + (\alpha_1 - \alpha_2)\Delta T\right] \qquad ...(19)$$

If we consider a single lap joint in which bending is restrained and if the thickness of the skin is t_s, then $t_1 = t_s / 2$.

4.2 2D F.E. analysis of a bonded joint

A 2D F.E. (plane stress) analysis has been carried out for a bonded joint whose geometry is shown in Fig.4. Only 2D isotropic, 8 noded quadrilateral elements are used in the analysis, and all lie in the xy plane. Fig.4 is a diagram only, but does indicate the areas in which the mesh is refined. Since a comparison is being made with the 1D d.e. which was developed earlier, the mesh contains only one element per structural component in the y direction.

In the thermal analysis the temperature has been set at a uniform temperature of 100°C throughout the joint. This is achieved efficiently by specifying the temperature at boundaries in such a way that the F.E. program completes the analysis by interpolation. The relevant thermal properties are coefficients of thermal expansion, α_1 and α_2, for components 1 and 2 given in Table 5. While the adhesive also has a thermal coefficient of expansion, this is set to zero to enable the best comparison with the 1D d.e. Also, it has been found that for PAFEC, non-zero conductivities must be set for isotropic elements. In steady state problems the actual value of the conductivity has no influence on the results provided it is not zero.

In the structural analysis that follows the corresponding 'structural' elements are used and the material properties used are given in Table 5. In the analysis the restraints used are:

1) restraints are used in the x direction for all nodes located on component 1 with co-ordinates of x = 0

2) restraint in the y direction for all nodes in component 1 with the co-ordinate of y = 0.

The restraints in the y direction have been applied to prevent bending of component 1, so that a direct comparison can be made with the 1D d.e.. Also in this analysis no non-thermal loads have been applied.

From the results a comparison of shear stresses can be made in two ways. Firstly, the shear stresses are calculated using the displacements from the F.E. analysis together with equation (13). Secondly, the shear stress is taken directly from the F.E. results corresponding to the maximum value that occurs in the midplane of the adhesive. These results are shown in Table 6, for a range of E_2 / E_1 values, together with the values predicted by the 1D d.e. (It should be noted that while the ratio of E_2 / E_1 is being varied all other parameters remain the same.) As shown in Table 6, the midplane solution gives better agreement with the 1D d.e. than the solution obtained from displacements.

Overall the difference in results between the 2D F.E. and 1D d.e. do not necessarily indicate the existence of an error in either solution. Factors that may influence results are firstly the Poisson's ratio effect which is not considered in the 1D d.e. Secondly, in the F.E. analysis shear deformation occurs in all components of the joint, while in the 1D d.e. it only occurs in the adhesive. Furthermore, the F.E. analysis of bonded repairs in general shows a considerable variation in shear stress from the patch/adhesive interface to the plate/adhesive interface.

To achieve good results in the F.E. analysis a very fine mesh of 0.05mm increments has been required to pick up the rise from $\tau = 0$ to a maximum at up to 0.25 mm away from the end of the joint. In the case of the d.e. the formulation is such that the maximum value occurs at the end of the joint. Although results are not given here, the decay of the F.E. and d.e. differ slightly.

In the case just considered the F.E. analysis was confined to the analysis of isotropic materials. Now consider the case in which component 2 has orthotropic properties. Composite materials are orthotropic and bonded joints are often comprised of such materials. In the repair of cracked metallic structures, materials such as boron/epoxy laminates are used as reinforcement. Consider a 2D analysis in which E_X is the major modulus of the laminate and E_Y represents the modulus perpendicular to the laminate. In this case the shear modulus is taken as that for a unidirectional layer of boron/epoxy. Using typical properties for the boron/epoxy and making a comparison with the 1D d.e. on the basis of $E_2 = E_X$ gives the result shown in Table 6 labelled as 'orthotropic'. Comparison of the shear stresses obtained by the F.E. and 1D d.e. show that better agreement is obtained with the F.E. midplane values than those obtained using equation (13). Overall, the comparison with midplane values in Table 6 has shown agreement to within 6%.

4.3 3D bonded joints

A 3D F.E. thermal analysis, using 20 noded brick elements, has been carried out for the structure defined in Fig. 5, which is fully restrained at the right hand end. Also bending in the z direction has been restrained. In this case the structure is subject to a uniform temperature of 100° C. The resulting τ_{zx} shear stresses have been evaluated in the middle plane of the adhesive at locations A and B as shown in Fig. 5., and have been found to reach a maximum value at a distance of approximately 0.2mm away from the end of the joint.

Results shown in Table 7 correspond to an isotropic material but with a modulus equal to that of a boron/epoxy laminate. This is simply to make a comparison with the 1D d.e., and orthotropic results to be considered later. The coefficient of thermal expansion is taken to be 4.1×10^{-6} /°C as used previously. The results are shown in Table 7 in which the number of elements in the width of the patch has been increased to demonstrate convergence. At point A a stationary value has almost been achieved, however convergence has yet to occur at point B. Values of shear stress at point A (47.54 MPa, Table 7 are considerably higher than the corresponding result (32.19 MPa, Table6) from the 1D equation. The shear stress values at point B (34.59 Mpa, Table 7) are significantly closer to the 1D equation result. These results indicate that a significant Poisson's effect is evident in the 3D case. It is therefore considered appropriate to model the composite as an orthotropic material. A 3D orthotropic analysis will now be considered.

4.3.1 3D orthotropic joint

The material properties of the basic unidirectional laminate of boron/epoxy used in the 3D analysis are given in Table 8. For a thermal analysis of a multi-ply laminate it is necessary to compute the effective coefficients of thermal expansion in the material symmetry axes. Usually manufacturers' data will provide the longitudinal (α_1) and transverse (α_2) coefficient of thermal expansion for a unidirectional laminate. In this case the longitudinal coefficient of thermal expansion is a measure of the fibre property while the transverse coefficient is a measure of the resin property. The effective coefficients of thermal expansion in the material symmetry axes are given by:

$$\alpha_L = \frac{1}{n}\sum_{k=1}^{n}\left(\alpha_1 Cos^2\theta + \alpha_2 Sin^2\theta\right) \qquad ...(20)$$

$$\alpha_T = \frac{1}{n}\sum_{k=1}^{n}\left(\alpha_1 Sin^2\theta + \alpha_2 Cos^2\theta\right) \qquad ...(21)$$

where:

k	is the k^{th} ply
θ	is the angle of the k ply to the material symmetry axes
n	is the total number of plies.

Note that the derivation for equations (20) and (21) assumes a balanced lay-up and is restricted to in-plane loadings. It is , however, possible to derive an expression to cover all other cases. For a 3D laminate the out of plane coefficient of thermal expansion may be taken as being equal to the value α_2 in the unidirectional lay-up.

In Table 9 a comparison has been made between the coefficients of thermal expansion for a unidirectional laminate and a lay-up consisting of $[0_2,\pm 45,0_3]_S$. The overall effect of the Poisson's ratio and the lay-up is to produce an effective coefficient in the longitudinal direction (α_L) higher than the unidirectional lay-up and a transverse coefficient (α_T) lower than the unidirectional lay-up.

The results shown in Table 10 are for a configuration in which the patch is homogeneous orthotropic and representative of a $[0_2,\pm 45,0_3]_S$ lay-up in which the principal material symmetry axis is in the x direction. For the purpose of comparison with the 1D equation, the coefficient of thermal expansion in the x direction is taken as $4.1\times10^{-6}/^{o}C$, while the coefficient in the y direction is taken as zero. The number of elements used in the width of the patch have been found to have a small effect on the results. The maximum τ_{zx} shear stresses occur in the middle of the patch (point A) while the τ_{zx} shear stresses on the edge (point B) are slightly lower. The maximum stresses are slightly higher than those predicted by the 1D lap-joint equation. Although not tabulated, an analysis has been carried out for the same problem as previously considered but with coefficients of thermal expansion of $6.24\times10^{-6}/^{o}C$ in the x direction while the coefficient of thermal expansion in the y direction is taken to be zero. These results gave a 9.7% reduction in shear stresses compared to the results shown in Table 10. This intermediate step was carried out to allow a useful comparison to be considered next.

Results shown in Table 11 are for the same problem as previously but correspond to coefficients of thermal expansion of $6.24\times10^{-6}/^{o}C$ and $16.96\times10^{-6}/^{o}C$ in the x and y directions respectively. These results are 20% lower than the previous results in Table 10 and together with the reduction of 9.7% from the intermediate step indicate that an interaction is occurring between the Poisson's ratio effect, and the two coefficients of thermal expansion. Clearly a 3D analysis is significantly different to a 1D analysis when both longitudinal and transverse coefficients of expansion exist, however the 1D lap-joint equation gives very close agreement. A comparison of all of these results is seen more clearly in Fig. 6.

4.3.2 Peel stresses

Usually the end of a bonded patch is tapered such that the thickness of the boron reinforcement is small and for the case of boron would be approximately 0.127 *mm*. This will result in significantly lower peel and shear stresses. While peel stresses have not been validated here, closed form solutions are available, and are usually derived as a function of the shear stress, ref(4).

5. Residual stress in a bonded repair

5.1 Bonding process

The bonding of a high strength patch to a plate involves heating of the patch and adhesive, and localised heating of the plate. This bonding process may be carried out at a temperature of between 80 - 120°C depending on the type of adhesive, and may involve a duration of several hours. When cured the patch and plate is allowed to cool to room temperature. As a result of the cooling and the different coefficients of expansion between the patch and the plate, residual stresses will occur in the plate, patch and adhesive. If the thermal coefficient of expansion of the plate is greater than that of the patch, as in the case of aluminium in comparison to a boron patch, then tensile residual stresses will develop in the plate while compressive stresses will occur in the patch. If, however, the plate is rigidly restrained close to the patch and the effective coefficient of expansion of the plate is lower than the patch, the residual compressive stresses will exist in the plate and tensile stresses in the patch.

It should be noted that for analysis purposes the shear modulus of the adhesive must be taken as some average value. This is because the shear modulus of the adhesive in the cured state varies significantly with temperature.

The procedure outlined here will enable the calculation of residual plate and patch stresses, and adhesive shear and peel stresses. However the validation presented here will only involve the plate and patch radial stresses. The circular plate analysed in section 2 has been reinforced in the central region with a circular patch of radius $r = R_1$. For the F.E. analysis two cases have been considered. Firstly, the patch is superimposed over the plate elements and shares the same nodes. The patch is considered to be welded to the plate. An analytic approach will be used to validate these results. Secondly the adhesive has been included in the analysis as 3D elements while the plate and patch are included as 2D elements. In this case it is necessary to model the adhesive as a 3D element to allow the transmission of shear. Since the plate is reinforced on one side only, bending effects will occur. As a result it is necessary to restrain the bending effects so that a comparison with an analytical approach can be made.

5.2 Analytical expression for residual stresses in a bonded repair

In a bonded repair both the patch and plate are heated to the cure temperature T. In the case of a plate in which the edges are restrained, the heating gives rise to an initial stress in the plate before curing of the adhesive and cooling takes place. In the case of the patch no restraint exists and the initial stress is negligible. To compute the initial stress in the plate we have the following expressions for displacement and radial stress, from ref(2):

$$u = \frac{\alpha_1(1+\nu)}{r}\int_0^r Trdr + Cr \qquad ...(22)$$

$$\sigma = -\frac{\alpha_1(1+\nu)}{r^2}\int_0^r Trdr + \frac{E_1}{(1-\nu)}C \qquad ...(23)$$

from the boundary condition that $u = 0$ at $r = R_O$ we obtain the integration constant C. From this the general form for the radial displacements and stresses is:

$$u = \frac{\alpha_1(1+\nu)}{R_O}\left\{\frac{R_O}{r}\int_0^r Trdr - \frac{r}{R_O}\int_0^{R_O} Trdr\right\} \qquad ...(24)$$

$$\sigma = -\alpha_1 E_1\left\{\frac{1}{r^2}\int_0^r Trdr + \frac{1+\nu}{(1-\nu)R_O^2}\int_0^{R_O} Trdr\right\} \qquad ...(25)$$

Specifically for $r = R_I$ the displacement is given by:

$$u = \frac{\alpha_1(1+\nu)}{2.}R_I(T_I - T_O)\left\{1 + \frac{1}{2\,ln(R_I / R_O)}\left(1 - \frac{R_I^2}{R_O^2}\right)\right\} \qquad ...(26)$$

Specifically for $r \le R_I$ we have a constant state of stress given by:

$$\sigma = -\frac{\alpha_1 E_1}{2}\left\{T_I + \frac{(1+\nu)}{(1-\nu)}\left[T_O + \frac{(T_I - T_O)}{2\ln(R_I / R_O)}\left(\frac{R_I^2}{R_O^2} - 1\right)\right]\right\} \qquad ...(27)$$

Equation (27) gives the required initial stress. The only reason that an expression for displacements have been derived is a means of checking the F.E. results. Both analytical and F.E. results are contained in Table 12 for a circular plate of R_I = 162 mm. The material properties correspond to those for the plate given in Table 1. A comparison of F.E. and analytic results shows agreement to 5 significant figures for both displacements and stresses.

The second part to the solution of residual stresses involves the analysis of the plate and patch. We require the state of stress corresponding to a cooling of the plate and patch. If we start at a temperature 0°C corresponding to zero initial stress, then cooling to a negative temperature equal in magnitude to the cure temperature $(-T)$ will give the required stress components. A summation with the initial stresses will give the residual stress state.

In this analysis, the adhesive will not be considered, and the patch is assumed to be rigidly connected to the plate. Radial stresses and displacements will be obtained for

the skin and patch. Consider a plate shown in Fig.7, which has properties E_1, α_1, t_1 for $r \geq R_I$ and overall properties E_o, α_o, t_o for $r \leq R_I$. Again the temperature boundary conditions are given by T_I being constant for $r \leq R_I$ and $T = T_O$ at $r = R_O$. The displacements are given by:

for $r \geq R_I$

$$u_1 = \frac{\alpha_1(1+\nu)}{r}\int_{R_I}^{r} Trdr + C_2 r + \frac{C_3}{r} \qquad ...(28)$$

for $r \leq R_I$

$$u_o = \frac{\alpha_o(1+\nu)}{r}\int_{0}^{r} Trdr + C_1 r \qquad ...(29)$$

The stresses are given by:

for $r \geq R_I$

$$\sigma_1 = -\frac{\alpha_1 E_1}{r^2}\int_{R_I}^{r} Trdr + \frac{E_1}{(1-\nu^2)}\left[C_2(1+\nu) - \frac{C_3(1-\nu)}{r^2}\right] \qquad ...(30)$$

for $r \leq R_I$

$$\sigma_O = -\frac{\alpha_O E_O}{r^2}\int_{0}^{r} Trdr + \frac{E_O}{(1-\nu^2)}C_1(1+\nu) \qquad ...(31)$$

The solution of these equations must satisfy the following conditions:

(a) The displacement u_1 and u_o is equal at $r = R_I$, hence from equations (28) and (29):

$$C_2 r + \frac{C_3}{r} = \frac{\alpha_o(1+\nu)}{R_I}\int_{0}^{R_I} Trdr + C_1 R_I \qquad ...(32)$$

(b) Equilibrium must be maintained across the boundary at $r = R_I$, using equations (30) and (31):

$$\frac{E_1 t_1}{(1-\nu^2)}\left[C_2(1+\nu) - \frac{C_3(1-\nu)}{R_I^2}\right] = -\frac{\alpha_o E_o t_o}{R_I^2}\int_{0}^{R_I} Trdr + \frac{E_o t_o}{(1-\nu)}C_1 \qquad ...(33)$$

(c) Also we have the further boundary condition that at $r = R_O$:

$$u_1 = 0 = \frac{\alpha_1(1+\nu)}{R_O}\int_{R_I}^{R_O} Trdr + C_2 R_O + \frac{C_3}{R_O} \qquad ...(34)$$

At this stage we have enough information for the evaluation of the constants C_1, C_2 and C_3.

It is more convenient to have the equations in the form that represent a patch over the skin for $r \le R_I$ as shown in Fig. 7. As before, the skin has the properties E_1, t_1, α_1 while the patch has the properties E_2, t_2, α_2. It is necessary to derive an expression for α_o in terms of these quantities. From equilibrium considerations we have :

$$E_o t_o \alpha_o = (E_1 t_1 + E_2 t_2)\alpha_o = E_1 t_1 \alpha_1 + E_2 t_2 \alpha_2 \qquad ...(35)$$

hence:

$$\alpha_o = \frac{(\alpha_1 + s\alpha_2)}{(1+s)} \qquad ...(36)$$

where:

$$s = \frac{E_2 t_2}{E_1 t_1} \qquad ...(37)$$

The expression for the stress state in the plate just outside the patch is given by equation (30) for $r = R_I$:

$$\sigma = E_1\left[\frac{C_2}{(1-\nu)} - \frac{C_3}{(1+\nu)R_I^2}\right] \qquad ...(38)$$

We will now derive the expressions for the stress state in the plate beneath the patch and in the patch. From equation (29) with $r \le R_I$, under a uniform temperature, the displacement is given by:

$$u = \left[\frac{(1+\nu)\alpha T_I}{2} + C\right]r \qquad ...(39)$$

Since the displacement is the same in both the patch and skin we have:

$$\frac{(1+\nu)\alpha_1 T_I}{2} + C_1 = \frac{u}{R_I} \qquad ...(40)$$

$$\frac{(1+\nu)\alpha_2 T_I}{2} + C_2 = \frac{u}{R_I} \qquad ...(41)$$

where the displacement u corresponds to the location $r = R_I$

The radial stresses for the plate and patch are given by:

$$\sigma_1 = -\frac{\alpha_1 E_1}{r^2}\int_0^r T_I r dr + \frac{E_1 C_1}{(1-\nu)} \qquad ...(42)$$

$$\sigma_2 = -\frac{\alpha_2 E_2}{r^2}\int_0^r T_I r dr + \frac{E_2 C_2}{(1-\nu)} \qquad ...(43)$$

Using equations (40), (41), (42) and (43) we have the expressions for the radial stresses in the plate beneath the patch and in the patch:

$$\sigma_1 = \frac{E_1}{(1-\nu)}\left[-\alpha_1 T_I + \frac{u}{R_I}\right] \qquad ...(44)$$

$$\sigma_2 = \frac{E_2}{(1-\nu)}\left[-\alpha_2 T_I + \frac{u}{R_I}\right] \qquad ...(45)$$

A circular plate with a patch has been considered in which the region $R_I = 162\ mm$ has been cooled down by a temperature of -100°C and the outer boundary has been set to 0°C. The material properties correspond to those in Table 4. Results for the analytical solution of equations (38), (44) and (45) are shown in Table 13 together with the F.E. results. Displacements agree to five significant figures. Values of stress in the patch and beneath the patch, agree to five significant figures. However the agreement of stresses in the plate just outside the patch varies from four significant figures at R_O = 500 *mm* to two significant figures at R_O = 5000 *mm*. This is entirely due to the 'stretched' F.E. mesh at the larger radius.

To obtain the residual stress in the plate beneath the patch it is necessary to sum equations (27) and (44), but with $T_I = -T_I$ in equation (44). Hence the final expression for the residual stress beneath the patch is:

$$\sigma = -\left(\frac{\alpha_1 E_1}{2}\right)\left\{T_I + \frac{(1+\nu)}{(1-\nu)}\left[T_O + \frac{(T_I - T_O)}{2\ln(R_I/R_O)}\left(\frac{R_I^2}{R_O^2} - 1\right)\right]\right\} + \frac{E_1}{(1-\nu)}\left(\alpha_1 T_I + \frac{u}{R_I}\right) \qquad ...(46)$$

Since the initial stress in the patch is zero, then the residual stress in the patch is given by equation (45), but again with $T_I = -T_I$ hence:

$$\sigma = \frac{E_2}{(1-\nu)}\left(\alpha_2 T_I + \frac{u}{R_I}\right) \qquad ...(47)$$

and the final expression for the residual stress just outside the patch is given by the summation of equations (27) and (38), hence:

$$\sigma = -\frac{\alpha_1 E_1}{2}\left\{T_I + \frac{(1+\nu)}{(1-\nu)}\left[T_O + \frac{(T_I - T_O)}{2\ln(R_I / R_O)}\left(\frac{R_I^2}{R_O^2} - 1\right)\right]\right\}$$
$$+E_1\left[\frac{C_2}{(1-\nu)} - \frac{C_3}{(1+\nu)R_I^2}\right] \qquad ...(48)$$

These equations now give the residual stress in terms of the cure temperature T. If, for example, the cure temperature is 100°C and residual stresses are required at a temperature of -40°C, then this would correspond to a temperature of $T = +140$°C.

5.3 Comparison of F.E. and analytic results

The numerical solution of these equations has been achieved and the following quantities have been evaluated for the comparison with F.E. results:

(a) displacement at $r = R_I$

(b) residual stress just outside the patch at $r = R_I$

(c) residual stress in the skin beneath the patch (σ_1)

(d) residual stress in the patch (σ_2)

In a similar way, a summation of the F.E. results has been carried out to compute the same quantities above.

As previously mentioned, the solution for the initial stresses are contained in Table12. Also, the solution corresponding to a temperature change of -100°C is shown in Table 13. Finally the residual stresses, which are a summation of these two cases, are shown in Table 14.

The complete results in Table 14 correspond to a range of outer plate radii, R_O. In the case of the displacements agreement between the analytic and F.E. results is to five significant figures. In the case of the residual stress in the plate, just outside the patch, agreement varies from four significant figures at the lower outer radii to three significant figures at the larger outer radii. Values for the residual stress in the plate beneath the patch, and in the patch agree to four significant figures.

So far, the adhesive has not been considered in the analysis. However F.E. results have been obtained in which the patch and plate have been coupled using 3D adhesive elements. To make a useful comparison with the previous analytical work the bending of the plate has had to be restrained. The material properties of the adhesive

correspond to the adhesive parameters given in Table 5. A comparison of these results is shown in Table 15. The introduction of the adhesive has resulted in an error of only 2% in direct stresses, showing that the use of a closed form solution is sufficiently accurate for patch design.

6. Discussion on thermal stress analysis using PAFEC

6.1 Thermal stresses

As mentioned previously, thermal stress analysis is carried out in two steps. Firstly a thermal analysis is carried out using 'thermal' elements. Some of these elements are shown in Table 16, and the complete list is contained in the relevant PAFEC manuals, ref(3). In Table 17 an example control module is shown for a steady state temperature solution in which the computed temperatures are to be written to file HOT1. For the thermal part of the analysis no restraints or loads are applied to the structure. Boundary conditions are most easily specified as temperatures on nodes of the structure, however they can also be specified as heat flux or a combination of both but not each at the same node.

The temperature module contains the temperature boundary conditions at specified nodes. It could contain the temperature in the entire structure if required, but this is not so convenient. A heat flux module can also be used if necessary, but generally it is easier to specify temperatures. Any serious problem usually involves the specification of temperature at a large number of nodes. As a result use of the PUPPIES program, ref(5), is the only feasible approach to this problem. Use of this program allows temperature to be set, for example, on the circumference of a plate, or alternatively within a radius of the centre of the plate such as that analysed in section 3.

It should be noted that thermal elements may be orthotropic in that the thermal coefficient of expansion or conductivity may be different in different directions. The PAFEC thermal solution is carried out in phases 1, 2, 4, 6 and 7 and it is not necessary to go to phase 9.

After the thermal solution has been completed then the structural analysis is run. The equivalent control module for the structural analysis is shown in Table 17 and instructs PAFEC to read in the temperature file HOT1 from the thermal analysis. Clearly, in the structural analysis restraints must be specified, although applied loads are optional. Another module required in the structural run is shown in Table 18. This module is included exactly as shown, and signifies that a steady state temperature analysis is involved. The structural analysis must have the same number of nodes and elements as in the thermal solution, otherwise temperatures will be assigned to the wrong nodes.

6.2 Residual thermal stresses

For F.E. analysis there are several methods for calculating residual stresses. An outline of these methods is given below:

6.2.1 Method 1

Consider an example in which a boron/epoxy patch is bonded to an aircraft wing. Usually an F.E. analysis is carried out when a repair is being made to primary structure. The F.E. model involves the patch and underlying skin and sometimes includes spar elements. The most convenient analysis would involve the structural detail only, in which an effective coefficient of thermal coefficient of expansion is used for the plate being reinforced. Obviously, the reinforcement would be analysed with the actual coefficient of thermal expansion. The effective coefficient of thermal expansion can be obtained using equation (10), which is derived from a circular plate with fixed (and free) edge restraints for the case $R_O / R_I = 0$. Studies on circular plates indicate that this is an upper bound, and hence is conservative. In this case the residual stresses are obtained with a total of two PAFEC runs.

6.2.2 Method 2

If the structural model of the repair is sufficiently large that it is connected to large surrounding structural elements such as spars, then the residual stresses may be obtained as carried out in section 5. This procedure involves the calculation of the initial stress for skin area corresponding to the cure temperature. The second component involves the complete structure subjected to a temperature equal to the cure temperature but opposite in sign. Again the residual stresses are obtained as a summation of the two components. In this method the coefficients of thermal expansion are the real coefficients for each material and a total of four PAFEC runs would be required.

6.2.3 Comment on methods 1 and 2

If this analysis is to be used to obtain residual adhesive shear stresses, then the correct choice of modulus for the adhesive is important. The modulus of the adhesive varies significantly with temperature and properties based on the 'average' from cure to operating temperature should be used.

6.2.4 Method 3

This method is that in which the variable material option of PAFEC is used to simulate the entire bonding process and would involve only two PAFEC runs. However it has not been possible to run this option at present. Until this error in PAFEC is corrected, methods 1 and 2 are the only available options.

7. Conclusions

In this report the validation of the thermal stress analysis capability of PAFEC, for steady state temperature problems, has been carried out. The F.E. results obtained for the heated circular plate are identical to those given by the one dimensional analytical solution, since the solution is radially dependent only. Furthermore the results obtained for the residual stress are identical to the analytical solution. In the case of bonded joints small differences occur, as a result of the comparison of a two (and three) dimensional F.E. analysis with a one dimensional analytical solution. Use of the procedures developed in this report will enable very accurate assessments of the stress states in bonded joints.

8. Acknowledgment

The authors wish to acknowledge the assistance of Dr L.R.F. Rose in the preparation of this report.

9. References

1. Jones, R. and Callinan, R.J., Thermal considerations in the patching of Metal Sheets with Composite Overlays, J. Struct. Mech.,8(2),1981.

2. Timoshenko, S.P., and Goodier, J.N. Theory of Elasticity. Pages 442-443. Third edition. McGraw-Hill 1970.

3. Anon, Data preparation manual for PAFEC.

4. Hart-Smith, L.J., Adhesively -Bonded Double-Lap Joints. NASA CR 112235, Jan. 1973.

5. Anon, PUPPIES users manual version 1.91 Analysis Software Pty Ltd. Mar 1995.

6. Lubin, G., Handbook of Fiberglass and Advanced Plastic Composites. Van Nostrand Reinhold Company, 1969.

Table 1. Material properties.

	Thickness (mm)	Young's modulus (MPa)	Poisson's ratio
Plate (Aluminium)	1.0	71016.	0.3
Patch (Boron)	0.5	156000.	0.3
Adhesive (FM300)	0.254	2273.	0.35

Table 2. Thermal properties.

	Coefficient of thermal expansion (/^{0}C)	Conductivity (J/ms^{0}C)
Plate - Aluminium (α_1)	23.E-06	160.
Patch - Unidir. Boron (α_2)	4.1E-06	-

Table 3. Comparison of temperatures predicted by F.E. and analytical expression.

r (mm)	226.5	291.0	936.1	2118.7	3107.8	3967.9
Analytic	90.227	82.921	48.853	25.036	13.865	6.741
F.E.	90.227	82.920	48.854	25.036	13.865	6.741

Table 4. Comparison of effective coefficients of thermal expansion for heated circular plate. (R_I=162.mm)

R_O (mm)	Analytic α_{eff}	F.E. α_{eff}	% error
500.	9.01E-06	9.014E-06	0.0
750.	10.30E-06	10.30E-06	0.0
1000.	10.95E-06	10.95E-06	0.0
2000.	11.99E-06	11.99E-06	0.0
3000.	12.40E-06	12.40E-06	0.0
5000.	12.77E-06	12.77E-06	0.0

Table 5. Material properties for bonded joint. (α_1 = 23x10^{-6}/^{0}C, α_2 = 4.1x10^{-6}/^{0}C)

t_1 (mm)	t_2 (mm)	t_a (mm)	ν_1	ν_2	ν_a	E_1 (MPa)	G_a (MPa)
3.6	1.778	0.254	0.3	0.3	0.35	71016.	842.

Table 6. Maximum adhesive shear stress in a bonded joint ,midplane values in parenthesis. (α_1 = 23x10^{-6}/^{0}C, α_2 = 4.1x10^{-6}/^{0}C)

E_2 / E_1 (MPa)	D.E. (MPa)	F.E. (MPa)	% Difference (based on F.E. being correct)
1.0	27.43	28.84 (25.77)	5.1 (-6.1)
1.5	30.06	33.48 (30.15)	11.4 (-.3)
2.0	31.70	36.46 (33.20)	15.0 (-4.7)
2.2 (Orthotropic)	32.190	35.49 (31.09)	9.3 (3.5)

Table 7. 3D isotropic F.E. results for maximum adhesive shear stress, corresponding to a uniform temperature of 100 ^{0}C, (α_1 = 23x10^{-6} /^{0}C, α_2 = 4.1x10^{-6} /^{0}C)

Number of elements across width	2	4	6	8
Shear stress at A	48.43	47.69	47.54	47.56
Shear stress at B	36.95	35.03	34.59	34.36

Table 8. Properties of unidirectional Boron/epoxy, ref(6)

E_{11} (MPa)	E_{11} / E_{22}	ν_{12}	G (MPa)
207000	10.89	.21	4800

Table 9. Thermal expansion coefficients for unidirectional Boron/epoxy, and values computed for a Boron/epoxy laminate.

Coefficient of expansion (/^{0}C)	Unidirectional	$[0_2, \pm 45, 0_3]_s$
α_L (longitudinal)	4.1x10^{-6}	6.24x10^{-6}
α_T(transverse)	19.1x10^{-6}	16.96x10^{-6}

Table 10. 3D orthotropic F.E. results for maximum shear stress, corresponding for a uniform temperature of 100 ^{0}C, (α_1 = 23x10^{-6} /^{0}C, α_L = 4.1x10^{-6} /^{0}C, α_T = 0 /^{0}C)

Number of elements across width	2	4	6	8
Shear stress at A	37.59	37.90	37.95	37.91
Shear stress at B	36.74	36.05	35.37	34.72

Table 11. 3D orthotropic F.E. results for maximum shear stress for a uniform temperature of 100 ^{0}C, (α_1 = 23x10^{-6} /^{0}C, α_L = 6.24x10^{-6} /^{0}C , α_T = 16.96x10^{-6} /^{0}C)

Number of elements through width	2	4	6	8
Shear stress at A	30.19	30.28	30.30	30.26
Shear stress at B	30.19	30.00	29.82	29.60

Table 12. 2D circular plate: F.E. results for initial stress and displacement at cure temperature of 100 ^{0}C, α_1 = 23x10^{-6} /^{0}C (analytic values in parenthesis)

R_o (mm)	Displacement at r=R_I=162mm (mm)	Initial stress at r ≤ R_I = 162 *mm* (MPa)
500	0.14602 (0.14602)	-141.89 (-141.89)
750	0.16686 (0.16686)	-128.84 (-128.84)
1000	0.17741 (0.17741)	-122.24 (-122.24)
2000	0.19433 (0.19432)	-111.64 (-111.64)
3000	0.20082 (0.20082)	-107.57 (-107.57)
5000	0.20692 (0.20692)	-103.76 (-103.76)

Table 13. 2D isotropic circular plate with patch. Displacements and stresses corresponding to a temperature of -100 ^{0}C, α_1 = 23x10^{-6} /^{0}C, α_2 = 4.1x10^{-6} /^{0}C (analytic values in parenthesis)

R_O (mm)	Displacement at edge of patch (mm)	Stress just outside patch (MPa)	Stress in skin beneath patch (MPa)	Stress in patch (MPa)
500	-0.11499 (-0.11499)	127.93 (127.92)	161.33 (161.33)	-66.813 (-66.813)
750	-0.12618 (-0.12618)	113.22 (113.21)	154.32 (154.32)	-82.213 (-82.213)
1000	-0.13189 (-0.13189)	105.72 (105.71)	150.74 (150.74)	-90.067 (-90.066)
2000	-0.14125 (-0.14125)	93.476 (93.409)	144.88 (144.88)	-102.94 (-102.94)
3000	-0.14493 (-0.14493)	88.621 (88.507)	142.57 (142.56)	-108.01 (-108.01)
5000	-0.14843 (-0.14843)	84.082 (83.975)	140.38 (140.38)	-112.82 (-112.82)

Table 14. 2D isotropic circular plate with patch. Residual displacements and stresses, α_1 = 23x10^{-6} /^{0}C, α_2 = 4.1x10^{-6} /^{0}C (analytic values in parenthesis)

R_O (mm)	Displacement at edge of patch (mm)	Residual stress just outside patch (MPa)	Residual stress in skin beneath patch (MPa)	Residual stress in patch (MPa)
500	-0.11499 (-0.11499)	-13.96 (-13.97)	19.44 (19.44)	-66.813 (-66.813)
750	-0.12618 (-0.12618)	-15.62 (-15.63)	25.48 (25.48)	-82.213 (-82.213)
1000	-0.13189 (-0.13189)	-16.52 (-16.53)	28.50 (28.50)	-90.067 (-90.066)
2000	-0.14125 (-0.14125)	-18.164 (-18.23)	33.24 (33.24)	-102.94 (-102.94)
3000	-0.14493 (-0.14493)	-18.949 (-19.06)	35.00 (34.99)	-108.01 (-108.01)
5000	-0.14843 (-0.14843)	-19.678 (-19.79)	36.62 (36.62)	-112.82 (-112.82)

Table 15. 2D isotropic circular plate, patch. and 3D adhesive elements. Residual displacements and stresses, α_1 = 23x10^{-6} /^{0}C, α_2 = 4.1x10^{-6} /^{0}C (analytic values in parenthesis)

R_O (mm)	Displacement at edge of patch (mm)	Residual stress just outside patch (MPa)	Residual stress in skin beneath patch (MPa)	Residual stress in patch (MPa)
500	-0.11551 (-0.11499)	128.31 (127.92)	161.91 (161.33)	-65.532 (-66.813)

Table 16. Corresponding elements for thermal and stress analysis

Element	Thermal	Structural
2 noded flange	*39800*	*34400*
6 noded triangle	*39110 (39115)*	*36110 (36115)*
8 noded quadrilateral	*39210 (39215)*	*36210 (36215)*
20 noded brick	*39710 (39715)*	*37110 (37115)*

Table 17. Example CONTROL MODULES

Thermal Analysis	Structural Analysis
CONTROL *CALC.STEADY.TEMPS* *SAVE.TEMPS.TO.HOT1* *FULL.CONTROL* *TOLERANCE=10E-3* *PHASE=1,2,4,6,7* *CONTROL.END*	*CONTROL* *READ.TEMPS.FROM.HOT1* *FULL.CONTROL* *TOLERANCE=10E-3* *PHASE=1,2,4,6,7,9* *CONTROL.END*

Table 18. Additional module required for structural analysis

TIMES.FOR.THERMAL.STRESS.CALCULATION *TIME* *0*

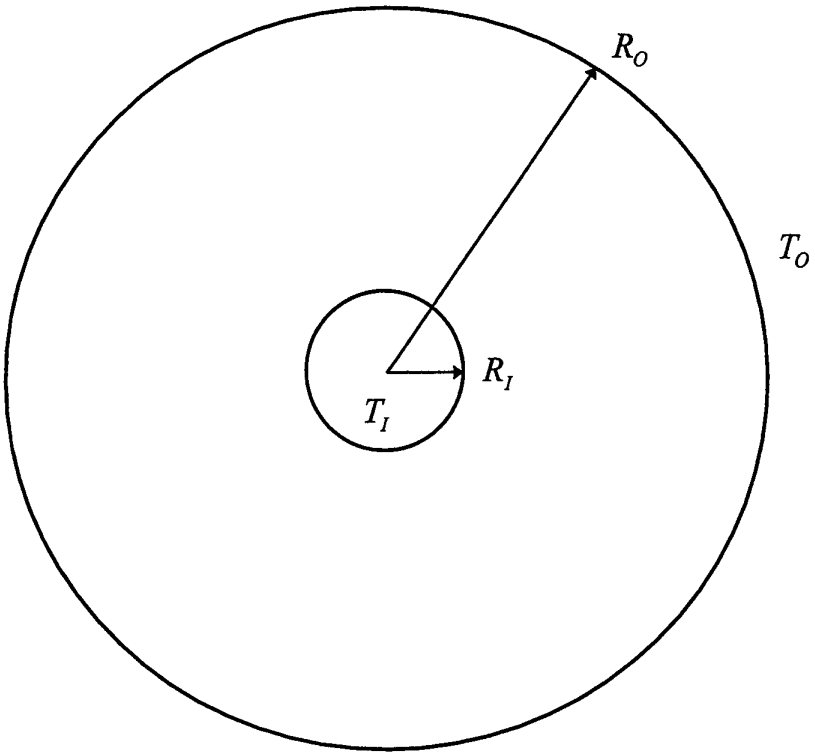

Figure 1. Circular plate, definition of parameters.

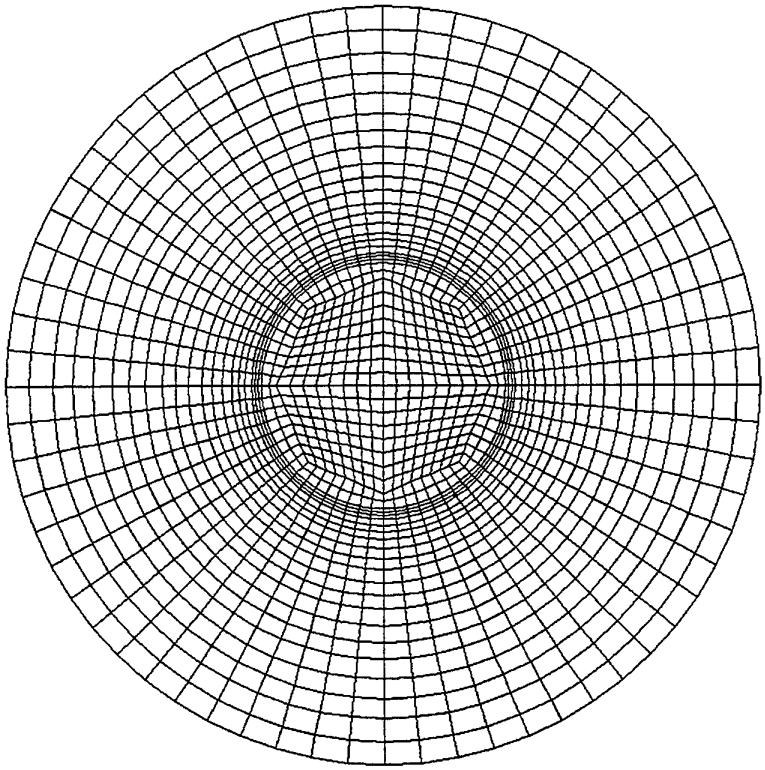

Figure 2. Finite Element mesh for plate, $R_I = 162mm$ and $R_O = 500mm$.

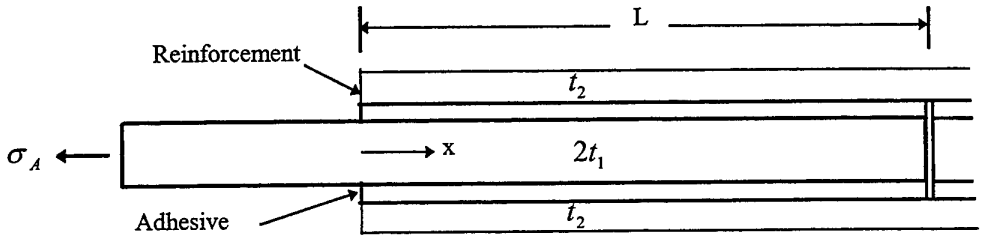

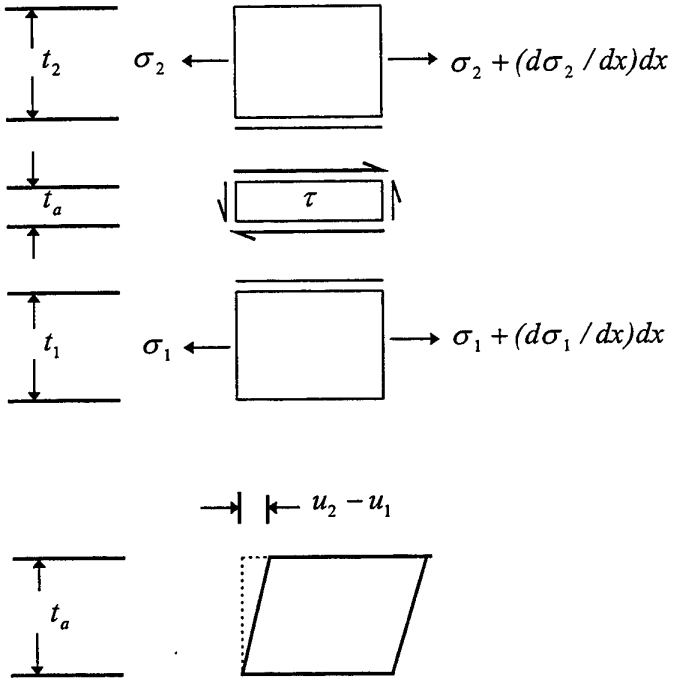

Figure 3. Definition of parameters for 1D bonded joint.

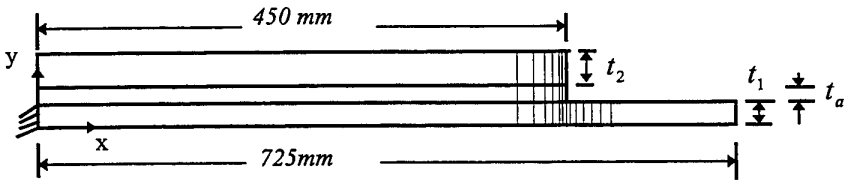

Figure 4. Definition of parameters for 2D bonded joint.

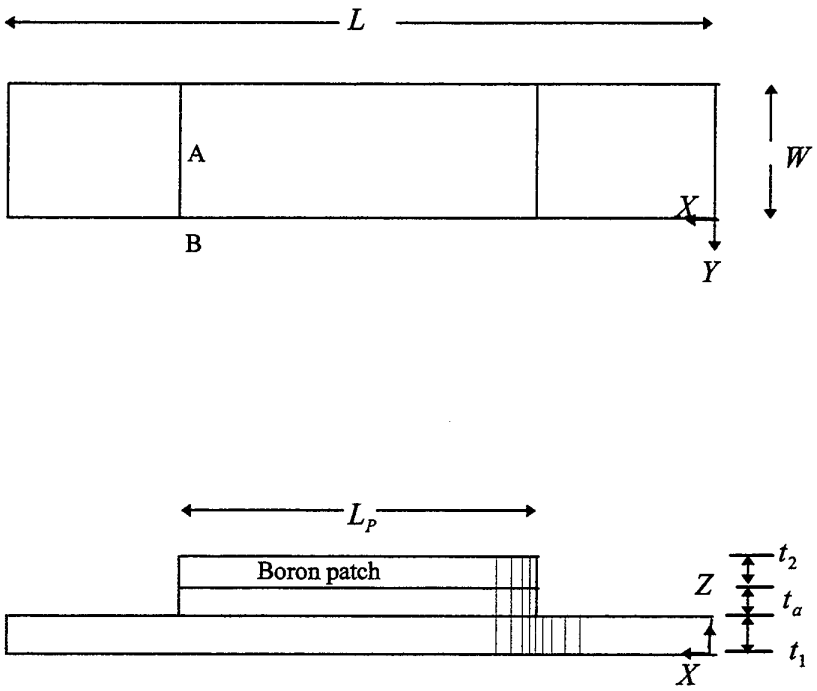

L=1000mm, L_P =450mm, W=450mm

Figure 5. Definition of parameters for 3D analysis of bonded joint.

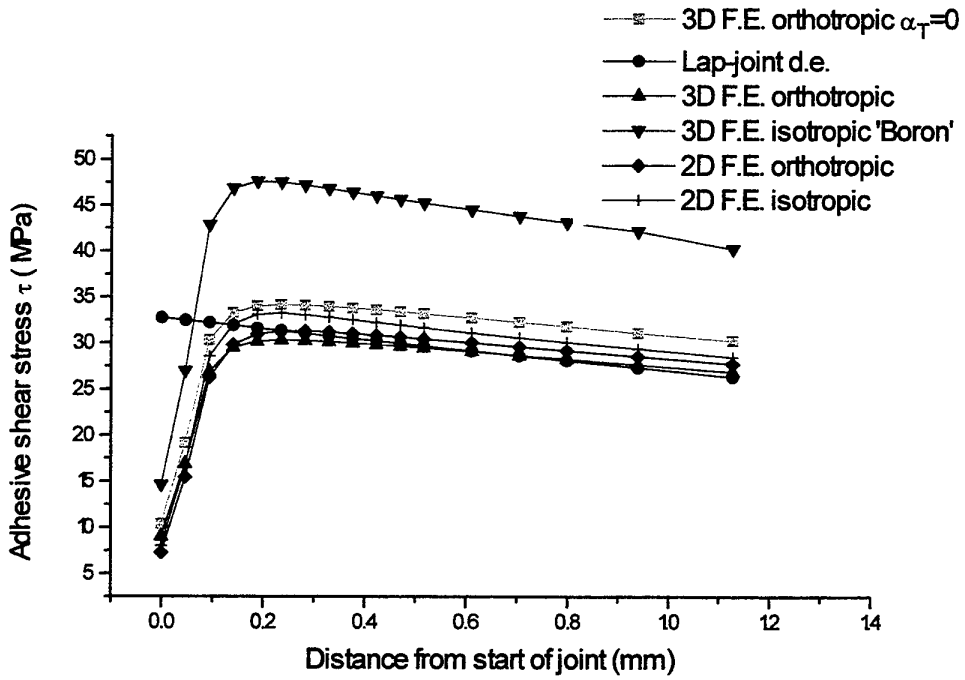

Figure 6. Comparison of adhesive shear stress for a range of cases.

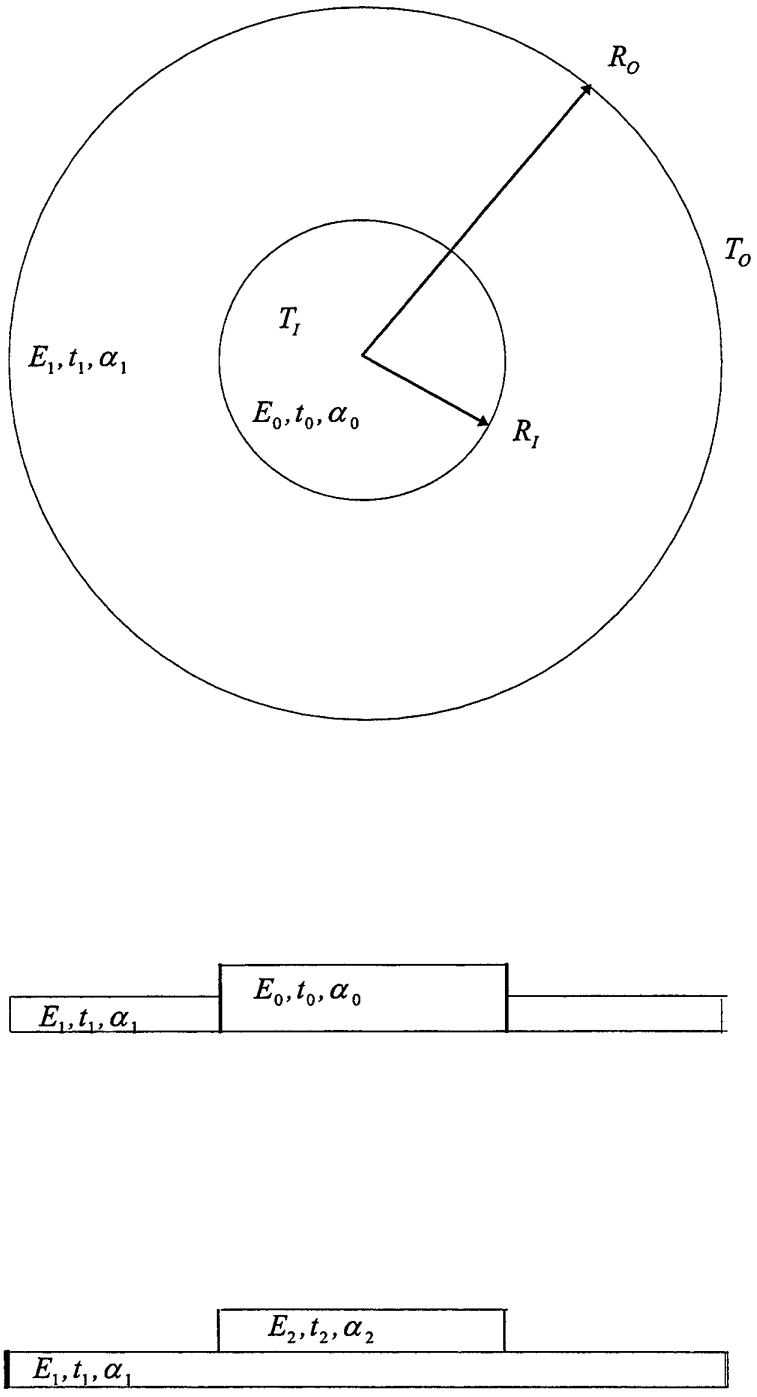

Figure 7. Equivalent circular plate for thermal residual stress problem.

DISTRIBUTION LIST

Development and Validation of a Finite Element Based Method to Determine Thermally Induced Stresses in Bonded Joints of Dissimilar Materials

R.J. Callinan, S. Sanderson, T. Tran-Cong and K. Walker

AUSTRALIA

DEFENCE ORGANISATION

Task Sponsor **DTA**

S&T Program

Chief Defence Scientist
FAS Science Policy
AS Science Corporate Management
} shared copy

Director General Science Policy Development
Counsellor Defence Science, London (Doc Data Sheet)
Counsellor Defence Science, Washington (Doc Data Sheet)
Scientific Adviser to MRDC Thailand (Doc Data Sheet)
Director General Scientific Advisers and Trials/Scientific Adviser Policy and Command (shared copy)
Navy Scientific Adviser (Doc Data Sheet and distribution list only)
Scientific Adviser - Army (Doc Data Sheet and distribution list only)
Air Force Scientific Adviser
Director Trials

Aeronautical and Maritime Research Laboratory
Director

Chief of Airframes and Engines Division
F. Rose
K. Walker
R.J. Callinan
S. Sanderson
T. Tran-Cong

DSTO Library
Library Fishermens Bend
Library Maribyrnong
Library Salisbury (2 copies)
Australian Archives
Library, MOD, Pyrmont (Doc Data sheet only)
Library, MOD, HMAS Stirling (Doc Data sheet only)

Capability Development Division
Director General Maritime Development (Doc Data Sheet only)
Director General Land Development (Doc Data Sheet only)
Director General C3I Development (Doc Data Sheet only)

Army

ABCA Office, G-1-34, Russell Offices, Canberra (4 copies)
SO (Science), DJFHQ(L), MILPO Enoggera, Queensland 4051 (Doc Data Sheet only)
NAPOC QWG Engineer NBCD c/- DENGRS-A, HQ Engineer Centre Liverpool Military Area, NSW 2174 (Doc Data Sheet only)

Air Force

Intelligence Program

DGSTA Defence Intelligence Organisation
Library, Defence Signals Directorate (Doc Data Sheet only)

Corporate Support Program (libraries)

OIC TRS, Defence Regional Library, Canberra
Officer in Charge, Document Exchange Centre (DEC), 1 copy
*US Defence Technical Information Center, 2 copies
*UK Defence Research Information Centre, 2 copies
*Canada Defence Scientific Information Service, 1 copy
*NZ Defence Information Centre, 1 copy
National Library of Australia, 1 copy

UNIVERSITIES AND COLLEGES

Australian Defence Force Academy
Library
Head of Aerospace and Mechanical Engineering
Deakin University, Serials Section (M list), Deakin University Library, Geelong, 3217
Senior Librarian, Hargrave Library, Monash University
Librarian, Flinders University

OTHER ORGANISATIONS

NASA (Canberra)
AGPS

OUTSIDE AUSTRALIA

ABSTRACTING AND INFORMATION ORGANISATIONS

INSPEC: Acquisitions Section Institution of Electrical Engineers
Library, Chemical Abstracts Reference Service
Engineering Societies Library, US
Materials Information, Cambridge Scientific Abstracts, US
Documents Librarian, The Center for Research Libraries, US

INFORMATION EXCHANGE AGREEMENT PARTNERS

Acquisitions Unit, Science Reference and Information Service, UK
Library - Exchange Desk, National Institute of Standards and Technology, US
National Aerospace Laboratory, Japan
National Aerospace Laboratory, Netherlands

SPARES (10 copies)

Total number of copies: 58

DEFENCE SCIENCE AND TECHNOLOGY ORGANISATION
DOCUMENT CONTROL DATA

1. PRIVACY MARKING/CAVEAT (OF DOCUMENT)

2. TITLE

Development and Validation of a Finite Element Based Method to Determine Thermally Induced Stresses in Bonded Joints of Dissimilar Materials

3. SECURITY CLASSIFICATION (FOR UNCLASSIFIED REPORTS THAT ARE LIMITED RELEASE USE (L) NEXT TO DOCUMENT CLASSIFICATION)

Document	(U)
Title	(U)
Abstract	(U)

4. AUTHOR(S)

R.J.Callinan, S. Sanderson, T. Tran-Cong and K.Walker

5. CORPORATE AUTHOR

Aeronautical and Maritime Research Laboratory
PO Box 4331
Melbourne Vic 3001 Australia

6a. DSTO NUMBER	6b. AR NUMBER	6c. TYPE OF REPORT	7. DOCUMENT DATE
DSTO-RR-0109	AR-010-236	Research Report	June 1997

8. FILE NUMBER	9. TASK NUMBER	10. TASK SPONSOR	11. NO. OF PAGES	12. NO. OF REFERENCES
M1/9/170	AIR94/118	DTA	24	6

13. DOWNGRADING/DELIMITING INSTRUCTIONS

None

14. RELEASE AUTHORITY

Chief, Airframes and Engines Division

15. SECONDARY RELEASE STATEMENT OF THIS DOCUMENT

Approved for public release

OVERSEAS ENQUIRIES OUTSIDE STATED LIMITATIONS SHOULD BE REFERRED THROUGH DOCUMENT EXCHANGE CENTRE, DIS NETWORK OFFICE, DEPT OF DEFENCE, CAMPBELL PARK OFFICES, CANBERRA ACT 2600

16. DELIBERATE ANNOUNCEMENT

No Limitations

17. CASUAL ANNOUNCEMENT Yes

18. DEFTEST DESCRIPTORS

finite element analysis, bonded joints, thermal stresses

19. ABSTRACT

A validation is carried out of the steady state thermal stress analysis capability of the PAFEC Finite Element program. Two problems are considered for which closed form solutions can be obtained: these comprise the thermal stresses in a heated circular plate and also a bonded joint. Also, a procedure is developed for calculation of residual stresses in bonded joints. Comparisons with closed form solutions indicate the degree of discretisation necessary to achieve accurate results.